



# Effects of *Chrysopogon zizanioides* root biomass and plant age on hydro-mechanical behavior of root-permeated soils

Kalani Rajamanthri<sup>1</sup> · Apiniti Jotisankasa<sup>1</sup> · Surachet Aramrak<sup>2</sup>

Received: 25 February 2021 / Accepted: 22 April 2021 / Published online: 11 May 2021  
© The Author(s), under exclusive licence to Springer Nature Switzerland AG 2021

## Abstract

Root biomass and plant age have been recognized to influence the hydro-mechanical properties of root-permeated soils, but its direct field observation was scarce. In this study, influences of *Chrysopogon zizanioides* (vetiver grass) of various plant ages (up to 2 years) on soil–water retention curves (SWRCs), saturated permeability, specific water–retention capacity and soil aggregate stability have been investigated. Undisturbed soil samples were obtained at different locations, representing the root zone, upslope, and downslope from the vetiver hedgerow at three bio-engineered slopes in Western Thailand. As root biomass increased, air–entry suction of soil slightly decreased, and porosity significantly increased due to the formation of macropores and aggregated soil structure in the root zone (0–15 cm depth). Nevertheless, below the root zone (15–25 cm depth), the air–entry suction of soil increased with root biomass due to the occupancy of soil pores by roots. Saturated permeability shows a positive correlation with plant age in the root zone, while a slightly negative correlation was found below the root zone. The upslope and downslope soil samples showed a negative correlation due to the effect of sediment trap. The specific water retention capacity and soil aggregate stability became higher in the root zone and positively correlated with plant age.

**Keywords** Soil bioengineering · Soil–water retention curve · Saturated permeability · Soil water retention capacity · Soil aggregate stability · Vetiver

## Introduction

Rain-induced shallow slope instabilities have become a frequently occurring hazard in various countries around the world [1]. In these slopes, shallow soil mass up to a depth of 1–3 m remains unsaturated during most time of the year. In such case, the apparent cohesion induced by negative pore water pressure, or soil suction, ensures the stability of the slope [2–4]. During prolonged rainfall events, the excess infiltration could create near-surface saturated zones which diminish the matric suction. The shear strength would subsequently decrease, resulting in shallow slope instabilities [5, 6]. The use of structural measures such as surface and subsurface drainage improvements to minimize infiltration

and to lower the groundwater table, construction of retaining structures to support collapsible mass, and internally stabilized systems have long been used to prevent these slope instabilities [7–9]. However, the application of vegetation for slope rectification is becoming popular among geotechnical engineers due to its low cost, aesthetic value, and sustainability [10–15]. Trees, shrubs, grasses, and various kinds of vegetation have been contributing to stabilize slopes for years. The main functions of vegetation in reducing landslide risk of a slope can be attributed to hydrological [10] and mechanical effects [11, 14], which are connected with the hydro-thermo and mechanical processes taking place in the soil [14–16]. Rainfall interception, evapotranspiration, and reduction in volume and velocity of surface runoff are some of the hydrological effects from vegetation. Hence, the vegetation has a significant impact on the behavior of the unsaturated zone of the slope subject to different climatic conditions. A number of researchers have investigated the mechanical effect of vegetation in enhancing the apparent cohesion by means of reinforcing the soil [14, 17]. Individual studies have shown different impacts of vegetation on

✉ Apiniti Jotisankasa  
fengatj@ku.ac.th

<sup>1</sup> Department of Civil Engineering, Kasetsart University, Jatujak, Bangkok 10900, Thailand

<sup>2</sup> Department of Soil Science, Kasetsart University, Jatujak, Bangkok 10900, Thailand

soil-water retention behavior [18–20], permeability [18–21] as well as soil aggregate stability (SAS) [22].

Vetiver grass (*Chrysopogon zizanioides*) is one of the extensively used plants for soil bio-engineering in tropical and subtropical countries [23–26]. Its applications vary from providing total nature-based solutions to forming hybrid systems as a component of structural measures. Normally, vetiver grass is planted as hedgerows parallel to the slope contours. The key feature of vetiver systems is its densely populated fine vertical root system which penetrates as deep as 3–4 m [27, 24–26]. Some recent studies have been aimed to assess the impact of vetiver grass root system on slope stability due to its efficacy for slope stabilization, reduction of runoff erosive energy, and sediment trap [12–15].

To quantify the vegetation effect on slope stabilization, the impact of the root system on soil hydraulic properties, i.e., soil-water retention curves (SWRCs), permeability functions are essential requirements. The root system has different effects during growing and decaying stages, and it is essential to capture the effects of roots in both stages [18]. Most studies show that actively growing roots could decrease both infiltration and saturated permeability [19–21], and decaying roots could increase these properties by creating preferential flow paths and macrospores [19]. In contrast, Leung et al. [28] recently reports that the growing roots could also increase the saturated permeability of a soil and plant age appeared to be a contributory factor. These contradictory findings warrant further studies in this area.

Vergani and Graf [22] have attempted to correlate the SAS with permeability using laboratory studies, but the results indicated no correlation between soil aggregate stability and permeability, probably due to the inadequate plant growth period. Significantly, Frei et al. [17] demonstrated that SAS is a critical indicator of plant growth, soil erosion, and it is directly related to the shear strength of the soil [17]. However, further studies are needed to investigate the impact of plant age on SAS.

In general, root-induced changes in hydraulic properties were frequently addressed using vegetated soil specimens that were developed under laboratory conditions [19, 21]. Plants, however, may behave differently in the field than in the laboratory-grown environment. Jotisankasa and Sirirat-tanachat [19] and Leung et al. [28] have observed some variations in terms of root diameter, root biomass, and relative root density subject to field and laboratory grown environment. In this study, an attempt has been made to assess the hydraulic properties, namely soil–water retention curves (SWRCs) and saturated permeability, of undisturbed soil samples collected from three selected sites in which vetiver grass has been grown as a measure of erosion control and slope stabilization. The selected sites, which were natural slopes, previously suffered from shallow slope instabilities, have been rectified using hybrid mitigation measures

involving geosynthetically reinforced soil (GRS) wall and bio-slope stabilization. Failures of some GRS walls due to soil erosion in the toe area has been reported in the literature [29]. Vetiver grass system has thus been used to improve slope stability and reduce soil erosion below the toe of GRS wall in these studied sites. Soil erosion phenomenon has a direct correlation with hydraulic flow behavior in root–soil systems and SAS [30]. This paper investigates the impact of root biomass and plant age on soil hydraulic properties and soil aggregate stability, using in situ collected undisturbed samples, which is seldom addressed by previous researchers.

## Materials and methods

### Materials

The materials used in this study were collected from side slopes of a rural road in Thong Pha Phum National Park, which suffered from mass movement and erosion in 2016 in Kanchanaburi Province, in Western Thailand (Fig. 1). The average inclination of the slopes with the horizontal plane is 45°. The road embankments were rebuilt using GRS walls to ensure the stability of the eroded slopes, namely Ithong 1, Ithong 2, and Ithong 3 where vetiver vegetation was also an integral part of the rectification system. Out of these three sites, Ithong 1 had the highest plant age (i.e., 623 days) at the time of sample collection, while Ithong 2, and Ithong 3 had the plant ages of 218 days, and 91 days, respectively.

Sampling was conducted in both disturbed and undisturbed forms. Sampling locations were selected to represent the differently grown root conditions. In order to obtain the undisturbed soil samples, a driven thin-wall tube sampler with a PVC liner inside, having an inner diameter of 63 mm and a height of about 50 mm was used. Two different layers were selected [upper layer (U): 0–15 cm and lower layer (L): 15–25 cm], and three samples were collected from each layer (Fig. 2). Two samples were collected at a distance of 20 cm from the vetiver plant representing both upper and lower layers in upslope (A) and downslope (B) directions. One sample was collected underneath the roots zone from both upper and lower layers (R) (Fig. 2). Table 1 shows the summary of sampling locations with sampling depths.

Disturbed samples were used to determine the basic soil properties. Soils were classified in accordance with the unified soil classification system (USCS) (Table 2). Figure 3 shows the particle size distribution curves obtained for all three sites. According to the USCS classification, Ithong 1 consists of poorly graded silty sand and samples collected from both Ithong 2 and Ithong 3 are classified as poorly graded clayey sand. They are all residual soil derived from the same geological unit of weathered interbedded shale and sandstone. Despite some variations in the fine contents of

**Fig. 1** Locations of studied slopes: Ithong 1, Ithong 2, and Ithong 3 (contours are shown only in soil bioengineered slope areas)

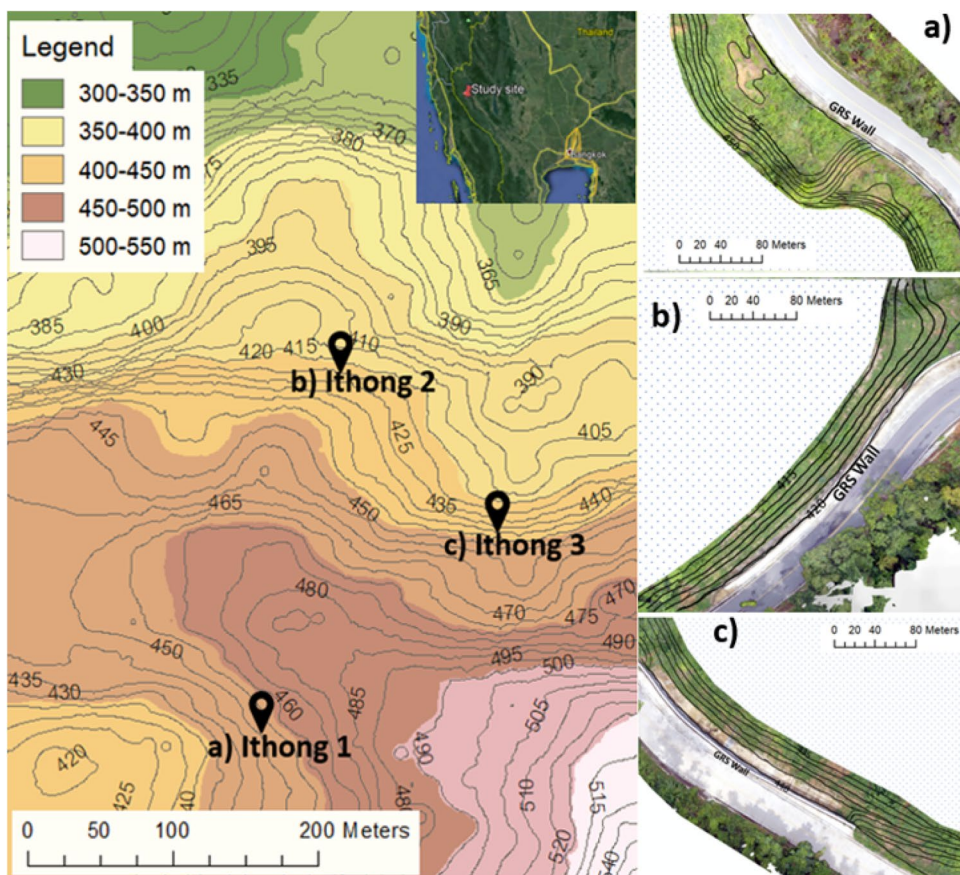


**Fig. 2** Schematic diagram of sampling location

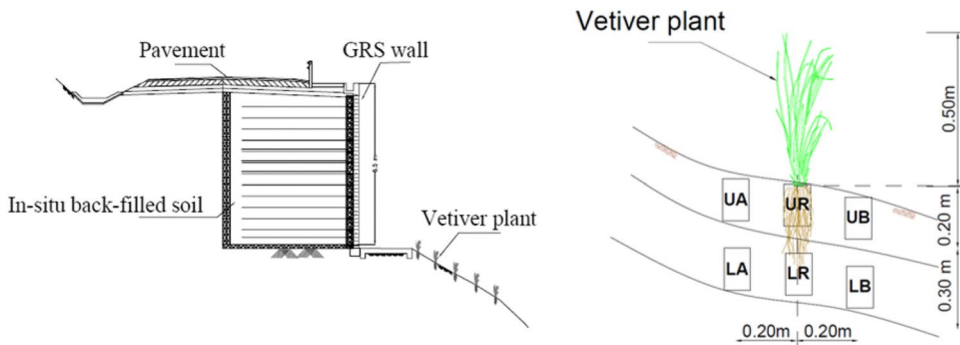


**Table 1** Summary of the sampling conducted

Symbol	Description	Depth
UA	Obtained from 20 cm away from the vetiver plant in the upslope direction	0–15 cm
UR	Obtained from the root zone	
UB	Obtained from 20 cm away from the vetiver plant in the downslope direction	
LA	Obtained from 20 cm away from the vetiver plant in the upslope direction	15–25 cm
LR	Obtained below the root zone	
LB	Obtained from 20 cm away from the vetiver plant in the downslope direction	

soils (4–8%) at these three sites, they were of similar properties, mainly consisting of sand-sized particles.

**Testing methods**

Test specimens (63 mm in diameter and 30 mm in height)

**Table 2** Properties of the material collected from three sites

Property	Site location			
	Ithong 1	Ithong 2	Ithong 3	
<b>Soil properties</b>				
Grain size distribution (%)				
Gravel (%)	(> 4.75 mm)	27.9	36.4	35.2
Sand (%)	(4.75–0.074 mm)	63.6	57.5	60.3
Silt (%)	(0.075–0.002 mm)	5.47	2.56	1.06
Clay (%)	(< 0.002 mm)	3.00	3.57	3.14
Specific gravity ( $G_s$ )		2.72	2.74	2.73
<b>Atterberg's limits</b>				
Liquid Limit, LL (%)		22.9	25.7	30.0
Plasticity Index, PI		2.91	3.97	5.82
Shrinkage limit, SL (%)		2.65	3.34	6.56
USCS	SP-SM	SP-SC	SP-SC	
<b>Dry density (kN/m<sup>3</sup>)</b>				
<b>Upper layer</b>				
UA	14.24	14.13	16.53	
UR	4.97	9.13	10.90	
UB	15.09	13.85	12.31	
<b>Lower layer</b>				
LA	15.32	14.53	*	
LR	14.29	13.03	13.67	
LB	15.10	12.94	14.40	
<b>Vegetation properties</b>				
Plant age (days) (beginning age was counted when onsite planting was completed)	623	218	91	
<b>Root biomass (kg/m<sup>3</sup>)</b>				
<b>Upper layer</b>				
UA	0.059	0.322	0.057	
UR	22.707	10.765	1.036	
UB	0.196	0.337	0.186	
<b>Lower layer</b>				
LA	0.172	0.063	*	
LR	0.486	0.245	1.241	
LB	0.197	0.193	0.000	

\*The specimen LA of Ithong 3 contained gravel particles larger than 10 mm and thus their presence affected the SWRC results and therefore omitted from interpretation. All the other samples's gravel particles were smaller than 10 mm

were prepared to determine the SWRCs for the wetting and drying paths. Miniature tensiometers (KU-T2 model) [2–4, 31] (Fig. 4a) were used to measure the soil suctions ranging from 0 to 80 kPa (Fig. 4). The wetting path was followed in the SWRC test (Fig. 4b) in the suction range between 0 and 100 kPa, which better represented the infiltration process during rainfall-induced landslide. However, the drying path was followed for suction above 100 kPa to obtain the complete SWRCs. It was noted that the soil suction as collected from the site for all samples was above 80 kPa. Therefore, samples were gradually wetted using a very

fine water spray. Once the sample's moisture content was increased as required, the sample was covered tightly in a sealed PVC container and cured 1–2 days for equilibration of soil suction throughout the soil sample [2–4, 6, 19]. After the suction was equilibrated, readings were taken, and the soil specimen's weight, dimensions were also measured for all samples at each wetting stage to acquire the data points of wetting SWRCs.

For the isopiestic technique (Fig. 4c) samples were equilibrated with total suction in the order of 14,029, 23,645, 39,370, and 365,622 kPa using saturated salt solutions of

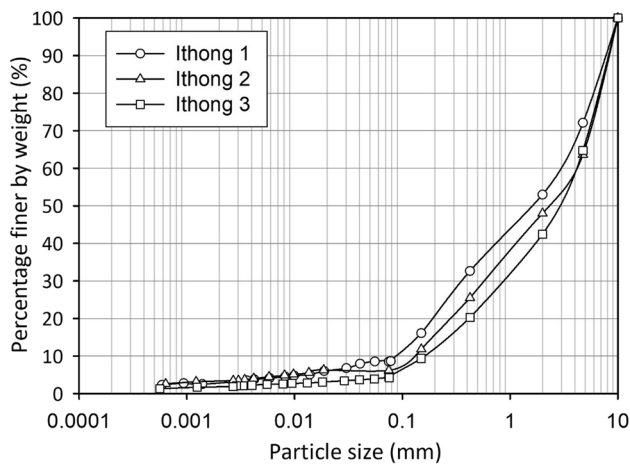


**Fig. 3** Particle size distribution curves for Ithong 1, 2, and 3

BaCl<sub>2</sub>, KCl, NaCl, and NaOH, respectively [3, 32, 33]. The attainment of suction equilibrium within a sample required about three weeks for each suction increment at this high suction range. The equilibrium was deemed to be reached, once the sample mass did not change more than 0.005%/day; thereafter, the final sample weight, dimensions and total suction were recorded. Notably, rainfall-induced slope instabilities normally involved suction values between 0 and 100 kPa, and therefore it was the tensiometer suction measurement that was the main focus of this experiment. However, to determine the curve fitting parameters based on Gitirana and Fredlund [34] (i.e., the residual suction, etc.), the isopiestic tests were conducted in a high suction range above 10,000 kPa.

Once the specimen achieved a soil suction of less than 0.5 kPa, the sample was soaked for 7–10 days to obtain a saturated sample (defined here as having the degree of saturation greater than 95%) with zero soil suction prior to the saturated permeability test. In this study, both constant

head and falling head testing methods were adopted by considering the fine content together with root content for each sample [19]. The testing procedure to determine the saturated permeability is similar to ASTM (2006) standard D2434 for coarse-grained soils (constant head method) and fine-grained soils (falling head method). To remove the air bubbles from the soil specimen, all samples were flushed with flowing water of about 1.5 m water head. Further, samples were subjected to a pressure head of 1.5–2.0 m throughout the testing to simulate the field condition with similar pore–water pressure when saturated or infiltrated with rainwater [19]. Prior to and during the testing, the water tightness of the system was carefully checked.

The trimmings of undisturbed soil samples were sieved to the aggregate diameter size of 1–2 mm and subsequently used for SAS testing. Before the test, soil specimens were moistened slowly to prevent the slaking effects (i.e., aggregate breakdown due to instantly wetting) using a closed chamber with the vapor above the saturated NaCl solution for 48 h, equivalent to vapor pressure at a field capacity [35]. The soil samples were then sieved using a wet sieving method with an opening of 250 μm at a constant rate of 35 revolutions per minute (Fig. 5). The soil samples which were passed through the sieve were considered unstable aggregate particles, and the retained soil particles were considered stable parts. Once the samples were separated, stable soil aggregates were destroyed to obtain sand particles, plant residues and organic matters by using a high-intensity ultrasonic processor [35]. Both stable and unstable samples were then placed in an oven at 105 °C to obtain the dry stable weight (*S*) and dry unstable weight (*U*). Equation 1 was used to calculate the SAS for each sample.

$$\%SAS = \frac{S}{(S + U)} \times 100. \quad (1)$$

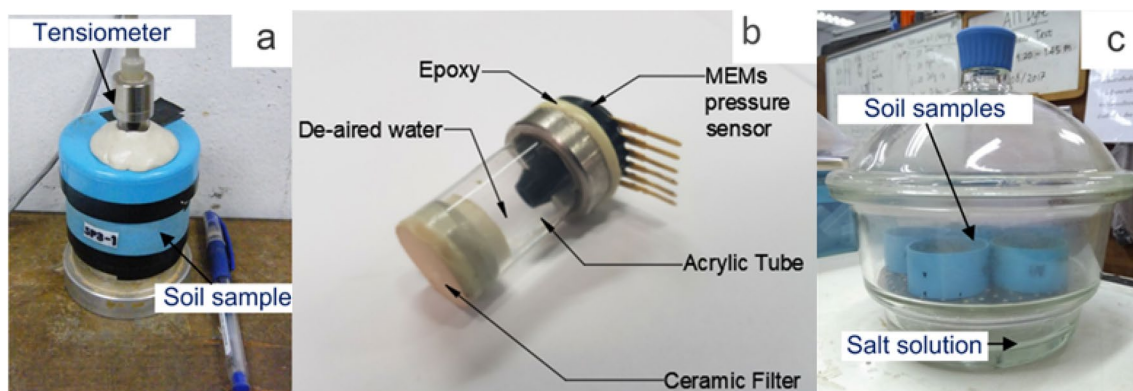
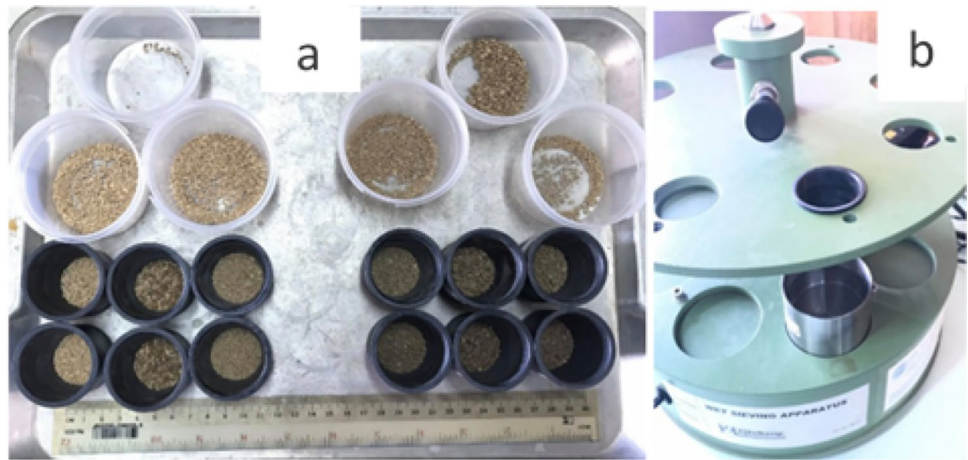


**Fig. 4** Photos of the experimental setup for obtaining SWRCs. **a** KU miniature tensiometer **b** suction measurement using KU miniature tensiometer **c** suction control using isopiestic technique

**Fig. 5** a) 250  $\mu\text{m}$  sieve set b) wet sieve apparatus for SAS



### Measurement of root contents

In this study, root mass in each sample were measured directly in terms of “dry root biomass per soil volume”,  $\rho_R$  ( $\text{kg}/\text{m}^3$ ). After the completion of all unsaturated soil property testing, sample was dismantled to measure the final moisture content and root content of the soil sample. In order to measure the root content, soil that was stuck with roots were washed carefully with water and passed through sieve number 20 (0.8 mm openings) to expose the roots. Roots that were passed through No. 20 sieve was considered as small and not included in root content measurements [19]. Roots which were retained on sieve No. 20 were oven-dried at 105 °C overnight to determine the dry biomass (measured to the precision of 0.001 gm) [36].

## Results and discussions

### Influence of roots on soil–water retention curves

Figures 6, 7, and 8 show the soil–water retention behavior for various undisturbed soil samples following the wetting and drying paths, which have different plant ages and root contents. To identify the impact of roots on soil–water retention behavior, different unsaturated soil parameters were determined: air entry value (AEV) and slope of the SWRC were obtained. AEV was obtained from the Gitirana and Fredlund model [34]. According to all three sites, it shows that all the samples that were obtained at the root zone at the upper layer (UR) have lower AEV, likely due to the large continuous voids of in situ soil, which are termed macro-pores.

The saturated volumetric water content of the root zone (UR) samples was clearly higher than the upslope (UA) and

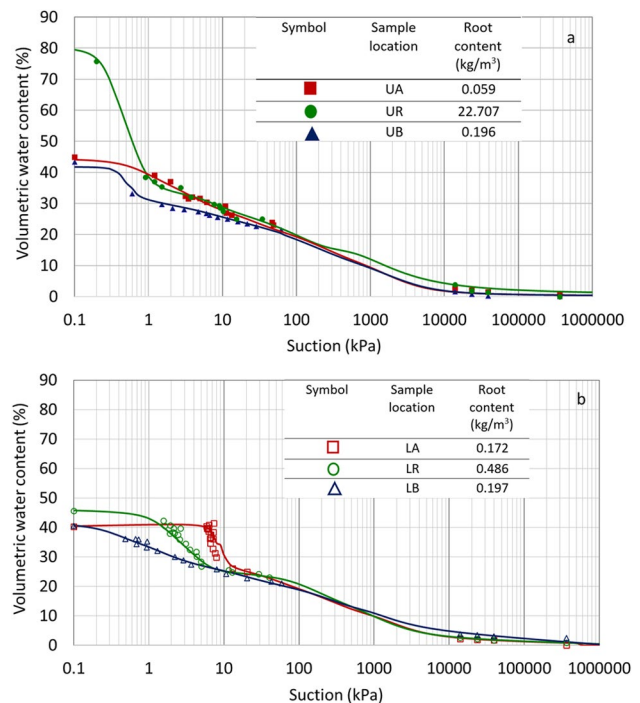


**Fig. 6** Soil water retention curves for Ithong 1 site **a** upper layer (U) and **b** lower layer (L)

downslope (UB) samples, indicating enhanced water-holding capacity around the roots. As for the lower layer soils of 15–25 cm depth, which were of lesser root contents, the air entry values appeared to increase as compared to the upper layer, which may also result from the higher relative density of the lower layer or roots occupying voids. Larger variations in SWRCs of the lower layer soils in different locations (LA, LR, and LB) can be observed and expected to be due to the intrinsic variability of the soil at the site and not due to the root effects.

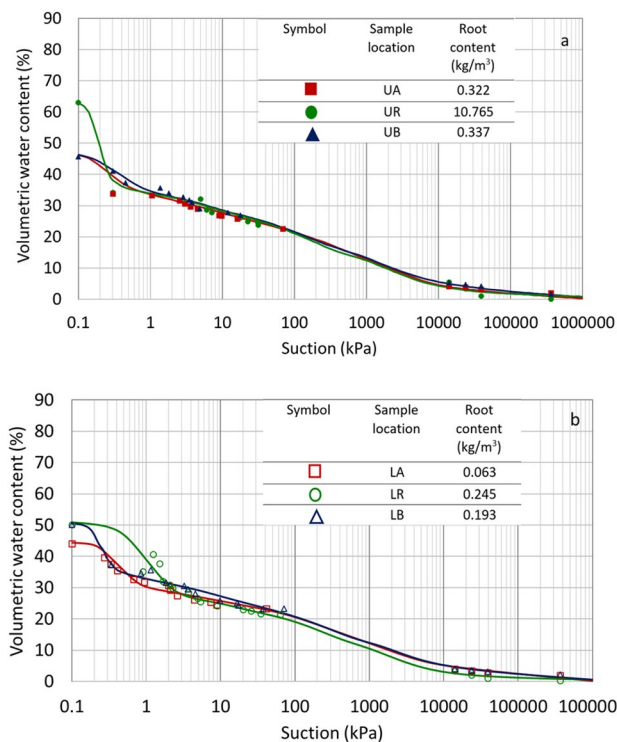


**Fig. 7** Soil water retention curves for Ithong 2 site **a** upper layer (U) and **b** lower layer (L)

The SWRCs obtained tend to have bimodal distributions. Hence, bi-modal SWRC equations proposed by Gitirana and Fredlund [34] were applied in this study to obtain the best fitting curves for SWRC as shown in Figs. 6, 7, and 8. This model was selected, considering its clear physical meaning with independent properties. As described in Fredlund and Gitirana [34] degree of saturation,  $S$  mainly depends on nine parameters, which are the SWRC features and the other one is the suction,  $\psi$ ,

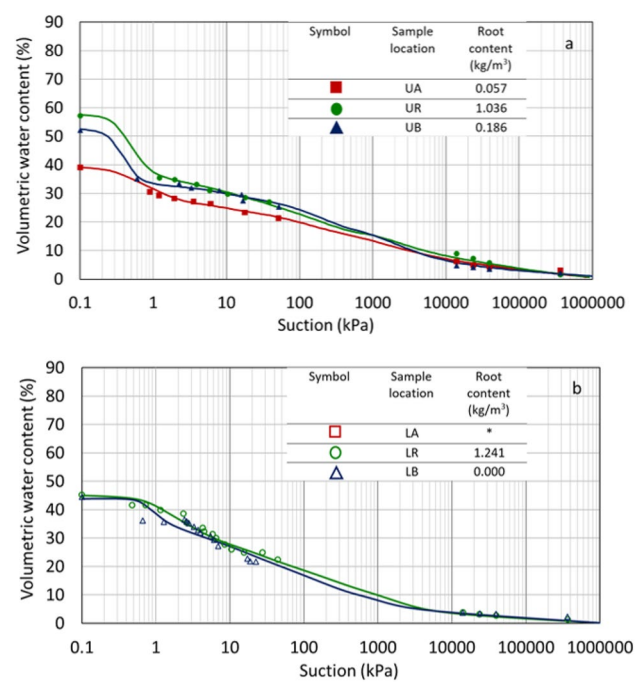


**Fig. 8** Soil water retention curves for Ithong 03 site **a** upper layer (U) and **b** lower layer (L)

$$S = f(\psi_{b1}, \psi_{res1}, S_{res1}, \psi_{b2}, S_b, \psi_{res2}, S_{res2}, a, S_{max}, \psi), \quad (2)$$

where  $\psi_b$  represents the air–entry suction of the drying SWRC or water–entry suction for wetting SWRC,  $\psi_{res}$  being the residual soil suction,  $S_{res}$  the residual degree of saturation, and  $a$  is the sharpness of the transitions at bending points. The subscripts 1 and 2 denote the two levels of soil structures.  $S_b$  is the degree of saturation at the air entry of the second structure level.  $S_{max}$  is the maximum degree of saturation upon soaking the sample during wetting which can be less than 100%. Gitirana and Fredlund’s formulation applies four hyperbolas to model the bimodal feature of SWRC in  $\log(\psi) - S$  coordinates. The degree of saturation can be calculated as follows:

$$S = S^* \times S_{max}, \quad (3)$$

$$S^* = \frac{S_1 - S_2}{1 + \left(\frac{\psi}{\sqrt{\psi_{b1}\psi_{res1}}}\right)^{d_1}} + \frac{S_2 - S_3}{1 + \left(\frac{\psi}{\sqrt{\psi_{res1}\psi_{b2}}}\right)^{d_2}} + \frac{S_3 - S_4}{1 + \left(\frac{\psi}{\sqrt{\psi_{b2}\psi_{res2}}}\right)^{d_3}} + S_4, \quad (4)$$

where,

$$S_i = \frac{\tan \theta_i (1 + r_i^2) \ln(\psi/\psi_i^a)}{(1 - r_i^2 \tan^2 \theta_i)} + (-1)^i \times \frac{(1 + \tan^2 \theta_i)}{(1 - r_i^2 \tan^2 \theta_i)} \sqrt{r_i^2 \ln^2(\psi/\psi_i^a) + \frac{a^2 (1 - r_i^2 \tan^2 \theta_i)}{(1 + \tan^2 \theta_i)}} + S_i^a;$$

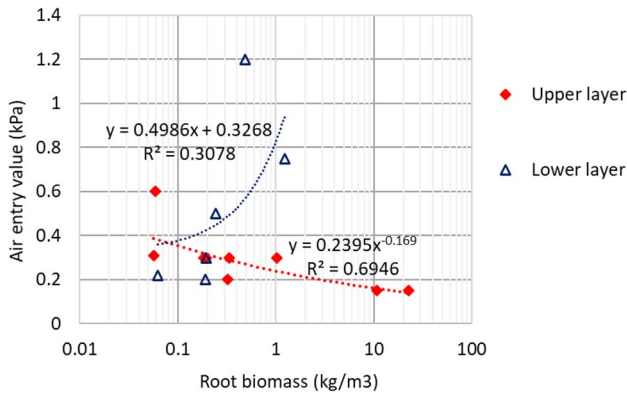


Fig. 9 Variation of air entry value with root biomass

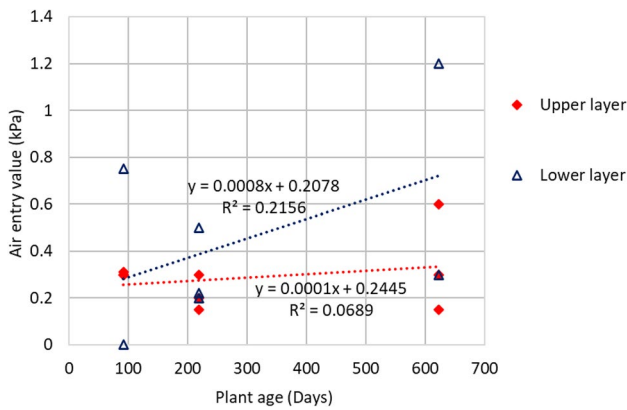


Fig. 10 Variation of air entry value with plant age

$i = 1, 2, 3, 4;$

$$\theta_i = -\frac{(\lambda_{i-1} + \lambda_i)}{2} = \text{hyperbolas rotation angles};$$

$$r_i = \tan \left[ (\lambda_{i-1} - \lambda_i) / 2 \right] = \text{aperture angles tangents};$$

$$\lambda_0 = 0; \lambda_i = \arctan \left\{ (S_i^a - S_{i+1}^a) / \left[ \ln \left( \frac{\psi_{i+1}^a}{\psi_i^a} \right) \right] \right\} = \text{desaturation slopes};$$

$$S_1^a = 1; S_2^a = S_{\text{res1}}; S_3^a = S_b; S_4^a = S_{\text{res2}}; S_5^a = 0;$$

$$\psi_1^a = \psi_{b1}; \psi_2^a = \psi_{\text{res1}}; \psi_3^a = \psi_{b2}; \psi_4^a = \psi_{\text{res2}}; \psi_5^a = 10^6;$$

$$d_j = 2 \exp \left[ 1 / \ln \left( \frac{\psi_{j+1}^a}{\psi_j^a} \right) \right] = \text{weight factor}; \text{ and } j = 1, 2, 3.$$

The variations in void ratios,  $e$ , with suction,  $\psi$ , during the tests were also calculated based on the measured volume and soil mass (Eq. 5). They were then used to determine the fitting curve for the volumetric water content–suction plots in Figs. 6, 7 and 8 as follows:

$$\theta(\psi) = \frac{e(\psi)}{1 + e(\psi)} S(\psi). \tag{5}$$

### Influence of root biomass and plant age on air–entry value suction

Figures 9 and 10 show the variations of air–entry value (AEV) suction with root biomass and plant age, respectively. According to Fig. 9, the upper layer samples, with a wider range of root biomass (up to 23 kg/m<sup>3</sup>), showed that air–entry suction decreased slightly with root biomass (negative correlation,  $R^2 = 0.6946$ ). This observation is similar to the findings by [19], who tested vetiver grass in laboratory conditions. This trend is believed to be due to the aggregate structure of the soil in the root zone. In contrast, the lower layer soil with a limited amount of roots (less than 1.5 kg/m<sup>3</sup>) showed a positive correlation, i.e., increasing air entry suction with root content, though with a poorer goodness of fit ( $R^2 = 0.3078$ ). This trend is similar to findings by [20] which represents actively growing roots without root decay. Figure 10 shows a rather scattered ( $R^2 = 0.0689$  and  $0.2156$ ) relationship for both upper and lower layers with respect to plant age. In this instance, both layers show a positive correlation between air entry value and plant age (Fig. 10), but the confidence level is considered much lower than the correlation with root biomass (Fig. 9). This is expected to be caused by intrinsic variation between plants of similar age. Accordingly, root biomass per soil volume is considered a better index for quantifying root influence on AEV than plant age.

### Quantify the effect of root biomass on curve fitting parameters of SWRC

As explained previously, root biomass per soil volume is considered a better index for quantifying root influence on soil–water retention behavior than plant age. Therefore, to incorporate the effect of roots on curve fitting parameters, Jotisankasa and Sirirattanachat [19] modified soil phase diagrams were considered together with root biomass and void ratio ( $e$ ). The proposed relationship takes into account soil grains, water, air, and roots (Eqs. 6, 7, and 8):



**Table 3** Curve fitting parameters for soil–water retention curves (SWRCs)

Sample location	$a$	$\psi_{b1}$ (kPa)	$\psi_{res1}$ (kPa)	$S_{res1}$	$\psi_{b2}$ (kPa)	$S_b$	$\psi_{res2}$ (kPa)	$S_{res2}$	$S_{max}$
Ithong 1—upper layer									
UA	0.08	0.60	7.0	0.57	100	0.5	4000	0.00005	0.98
UR	0.10	0.25	0.90	0.40	60	0.37	2500	0.00001	0.98
UB	0.08	0.43	0.60	0.74	84	0.53	5000	0.0005	0.99
Ithong 2—upper layer									
UA	0.05	0.15	0.40	0.75	220	0.46	7200	0.07	0.98
UR	0.09	0.15	0.25	0.55	80	0.44	5000	0.01	0.98
UB	0.09	0.20	0.55	0.70	60	0.58	4500	0.07	0.98
Ithong 3—upper layer									
UA	0.07	0.31	2.0	0.64	42	0.62	5000	0.145	0.98
UR	0.08	0.30	0.80	0.60	200	0.43	2500	0.15	0.99
UB	0.12	0.30	0.50	0.60	100	0.57	4000	0.005	0.98
Ithong 1—lower layer									
LA	0.10	7.50	10.0	0.62	200	0.48	3000	0.03	0.99
LR	0.09	1.20	6.5	0.50	70	0.57	2500	0.04	0.99
LB	0.09	0.30	2.0	0.64	200	0.49	2000	0.12	0.97
Ithong 2—lower layer									
LA	0.03	0.22	0.80	0.68	80	0.52	5500	0.12	0.99
LR	0.09	0.50	2.2	0.50	100	0.47	4500	0.01	0.99
LB	0.08	0.20	0.30	0.68	220	0.43	4000	0.07	0.99
Ithong 3—lower layer									
LR	0.05	0.75	5.0	0.65	150	0.44	3500	0.08	0.99
LB	0.05	0.65	1.20	0.78	200	0.35	1500	0.10	0.99

$$n = \frac{V_v}{V} = \frac{V - V_s - V_r}{V} = \frac{V - \frac{W_s}{G_s \gamma_w} - \frac{W_r}{G_r \gamma_w}}{V}, \tag{6}$$

$$e = \frac{V_v}{V_s} = \frac{V - V_s - V_r}{V_s} = \frac{V - \frac{W_s}{G_s \gamma_w} - \frac{W_r}{G_r \gamma_w}}{\frac{W_s}{G_s \gamma_w}}, \tag{7}$$

$$\theta = \frac{V_w}{V} = \frac{(W - W_r - W_s)}{\gamma_w} \frac{1}{V}, \tag{8}$$

where  $n$  defines as porosity;  $V$  is total volume;  $V_v$  is void volume;  $V_s$  is volume of soil particles;  $V_r$  is volume of roots;  $\gamma_w$  is water unit weight;  $G_s$  and  $G_r$  are the specific gravity of the soil grain and root, respectively;  $\theta$  is the volumetric water content;  $V_w$  is water volume;  $W$  is total weight;  $W_r$  is weight of roots;  $W_s$  is weight of soil particles. The value of root specific gravity was measured using the method similar to Leung et al. [27] and found to be about 0.604.

Table 3 summarizes the curve fitting parameters used in this study to construct the fitting curves in Figs. 6, 7, and 8. To establish a correlation between the SWRC shape and root biomass ( $\rho_R$ ) and void ratio ( $e$ ), multiple linear regression analyses are performed for each curve fitting parameters to obtain the relationships as follows:

$$a = \exp(-2.6571 + 0.6260 \ln e - 0.113 \ln \rho_R) \quad (R^2 = 0.3422), \tag{9a}$$

$$\psi_{b1} = \exp(-1.6732 + 1.0194 \ln e - 0.3571 \ln \rho_R) \quad (R^2 = 0.4780), \tag{9b}$$

$$\psi_{res1} = \exp(-1.094 + 2.5545 \ln e - 0.8410 \ln \rho_R) \quad (R^2 = 0.5133), \tag{9c}$$

$$S_{res1} = 0.7582 + 0.0014e - 0.1096\rho_R \quad (R^2 = 0.7137), \tag{9d}$$

$$\psi_{b2} = 1.7119 - 17.2252e - 128.0507\rho_R \quad (R^2 = 0.3029), \tag{9e}$$

$$S_b = 0.6115 + 0.0034e - 0.0932\rho_R \quad (R^2 = 0.5622), \tag{9f}$$

$$\psi_{res2} = \exp(8.6329 - 1.1476 \ln e + 0.2019 \ln \rho_R) \quad (R^2 = 0.6125), \tag{9g}$$

$$S_{res2} = \exp(-3.0616 - 8.8321 \ln e + 1.6221 \ln \rho_R) \quad (R^2 = 0.3055), \tag{9h}$$

$$S_{max} = 0.9709 - 0.0018e + 0.01276\rho_R \quad (R^2 = 0.3571). \tag{9i}$$

The void ratio ( $e$ ) was derived based on the modified phase relationships proposed by Jotisankasa and Sirirattachai [19] to account for the presence of roots in a soil and  $\rho_R$  is the dry root biomass which is a unit dependent. It

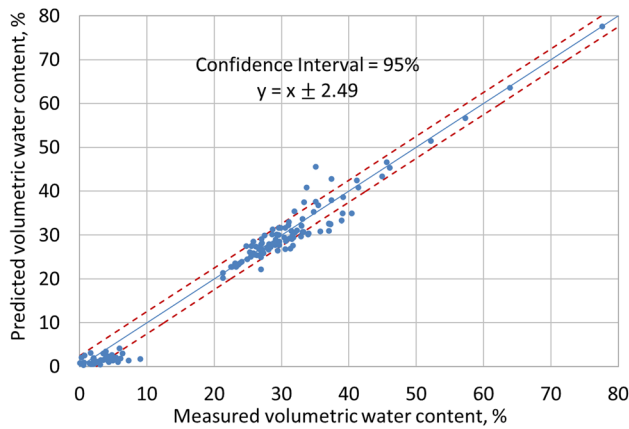


**Fig. 11** Comparison between predicted and measured moisture content

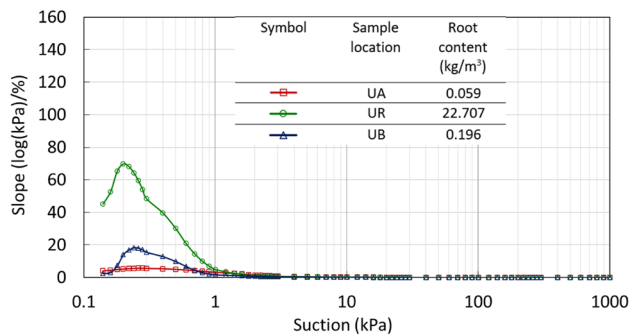


**Fig. 12** Water retention capacity at Ithong 1 site (plant age: 623 days)

can be seen that the correlation of  $\psi_{res1}$ ,  $S_{res1}$ ,  $S_b$ , and  $\psi_{res2}$  (Eqs. (9c), (9d), (9f), and (9g) with void ratio and root biomass were more satisfactory (of  $R^2$  varies between 0.5133 to 0.7137), and hence it can be concluded that those SWRC curve fitting parameters are dependent on the vegetation properties. Nevertheless, the  $R^2$  values obtained for other curve fitting parameters (i.e.,  $a$ ,  $\psi_{b1}$ ,  $\psi_{b2}$ ,  $S_{res2}$ , and  $S_{max}$  (Eqs. (9a), (9b), (9e), (9h), and (9i)) were found to range between 0.3055 and 0.4780, suggesting only moderate correlations amongst these parameters.

The volumetric water content during the SWRC test was predicted based on the onsite vegetation properties ( $e$  and  $\rho_R$ ) using the proposed relationship with the measurement as shown in Fig. 11. Only the upper root zone results were included in the analysis, while the results of lower layer soils were omitted due to the heterogeneity of the latter that would complicate the correlations. According to the obtained results, it shows a good agreement ( $R^2=0.9738$ ) with an error range of  $\pm 2.49\%$  volumetric water content based on the 95% confidence interval. This approach can be used for predicting SWRC based on the soil and vegetation properties (i.e.,  $e$  and  $\rho_R$ ) to be subsequently employed for seepage

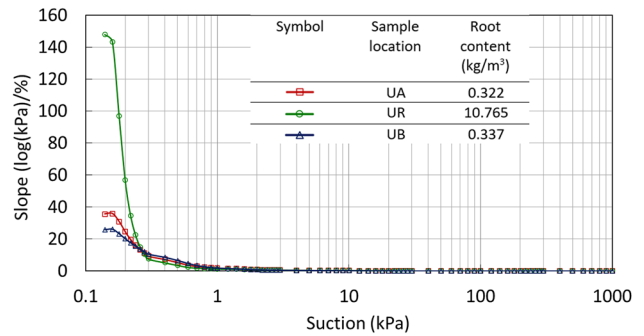


**Fig. 13** Water retention capacity at Ithong 2 site (plant age: 218 days)

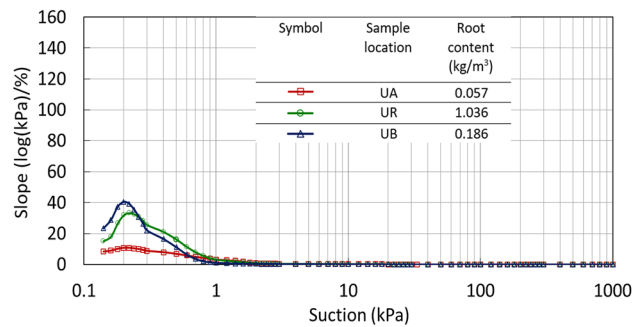


**Fig. 14** Water retention capacity at Ithong 3 site (plant age: 91 days)

analysis of bioengineered slopes of varying plant ages and root content in practice.

### Specific water retention capacity

Specific (or differential) water retention capacity ( $c_\theta$ ) describes the amount of storage or availability of water in the soil samples. This is derived from the slope of the soil-water retention curve, which is the change of volumetric water content per unit change in matric water potential (Eq. 10) [37];

$$c_\theta = \frac{-d\theta}{d\psi} \tag{10}$$

where  $d\theta$  is the change of volumetric water content in the soil sample and  $d\psi$  is the change in soil suction with respect to moisture change in the sample. Regression analysis was used in this study to calculate the slope of the SWRCs.

The specific water retention capacity mainly depends on the matric potential, soil's wetness, soil texture, and hysteresis [37]. Figures 12, 13, and 14 present the specific water retention capacity for each undisturbed soil sample at the upper layer (0–15 cm). When compared with

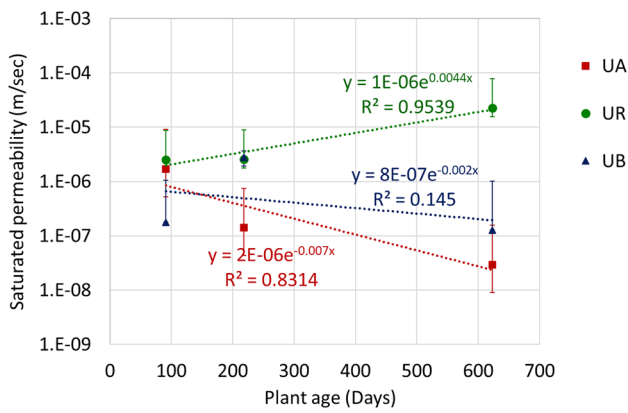


**Fig. 15** Variation of saturated permeability with plant age at upper layer (0–15 cm)

the UA and UB samples, root zone (UR) samples have a higher water retention capacity to store water. Generally, the specific water retention capacity of the root zone (UR) from more matured vetiver plants (Ithong 1: 623 days and Ithong 2: 218 days) was greater than that of younger vetiver (Ithong 3: 91 days). Theoretically, the steeper slope or higher water retention capacity at a suction range of 0.1–1 kPa corresponds to a macropore size range from 1.5 to 0.15 mm, which was the same as the size of grass roots. In general, vetiver grass is considered as one of the plants, which have a higher water retention capacity [25]. Further, as explained by Jotisankasa and Sirirattanachat [19], water retention around the roots would also be a function of the root exudation. These soil–plant–fungus interactions create biochemical cementation in between the soil particles and aggregates thus enhancing the water availability for the plants [17, 19]. This conjecture will be confirmed with SAS test results as will be presented later. Interestingly though, the Ithong 2 UR sample has a slightly steeper slope than Ithong 1 despite its younger age. The reason is unclear, but probably due to the regrowth of vetiver plants at Ithong 1 or natural variation among the plants.

**Influence of roots on saturated soil permeability**

Saturated soil permeability is a critical parameter in implementing soil bioengineering rectification measures for slopes [12, 13, 16, 38]. It directly influences the generation of runoff and subsurface pore water pressure [10, 11]. Figure 15 shows the variation of saturated permeability with three distinct plant ages at the upper layer (0–15 cm). The saturated permeability,  $k_{sat}$ , is obtained from the conventional testing methods (i.e., constant head and falling head apparatus). Further, to prevent the uncertainty in saturated permeability determination, the effect of temperature also was taken

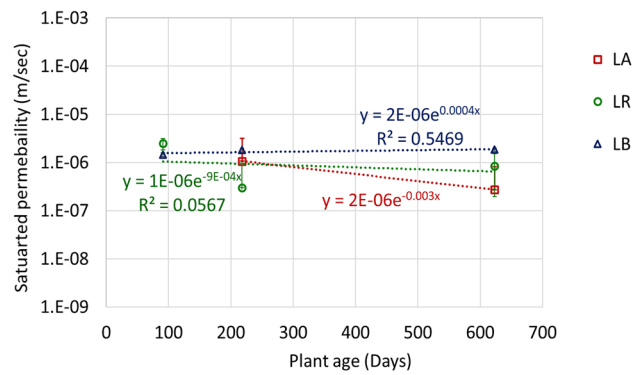


**Fig. 16** Variation of saturated permeability with plant age at the lower layer (15–25 cm)

into account and the standard temperature was considered as 20 °C [39];

$$k_{20} = k_T \left( \frac{\eta_T}{\eta_{20}} \right). \tag{11}$$

Further, trend lines and error bars for the saturated permeability values were determined in both Figs. 15 and 16 by considering the 80% confidence interval [19, 40]. Interestingly,  $k_{sat}$  value of the root zone (UR) samples shows a significant positive correlation ( $R^2 = 0.9539$ ) with plant age as compared to the other two locations (UA and UB). This finding agrees with those presented by Jotisankasa and Sirirattanachat [19] and Leung et al. [28] who tested the same grass (*Chrysopogon zizanioides*) and a willow species (*Salix viminalis tora*), respectively, and found also a positive correlation with the increment of root biomass and plant age. This may be due to aggregated structure developing with plant age and preferential flow paths or cycles of wetting and drying at the field. Preferential flow paths can occur due to the channels formed by dead or decaying roots, by decayed roots that are newly occupied by living roots and around live roots. In addition, root architecture also influences the preferential flow path [41]. However, the saturated permeability of UA and UB samples comparatively follow a negative correlation as compared to UR samples. This can be a consequence of the sediment trap at these two locations. In general, vetiver grass is categorized as one of the effective plants in trapping sediments [25]. Therefore, saturated permeability at these two locations (UA and UB) tends to decrease with time as more sediments were trapped behind the vetiver hedgerow.

Figure 16 shows the variation of  $k_{sat}$  with plant age for the lower layer (15–25 cm). In this study, the value of  $k_{sat}$  at all three locations (LA, LR, and LB) follows a similar trend, a slightly negative correlation with plant age, although a

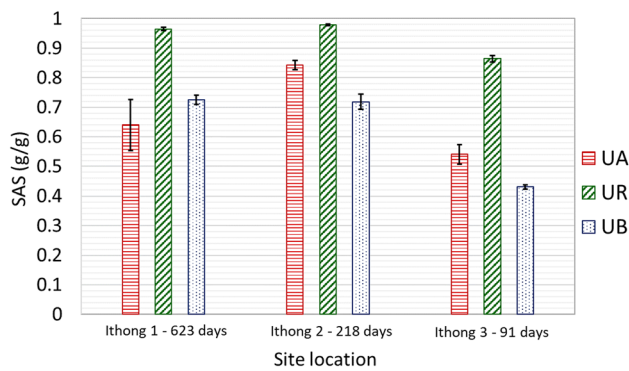


**Fig. 17** Variation of soil aggregate stability (SAS) with plant age

goodness of fit was generally lower. This may be due to roots occupying soil pores and natural variations between these sites. All in all, the smaller saturated soil permeability of the lower layer would be beneficial in terms of slope stability since it would inhibit the deeper infiltration that would consequently increase pore–water pressure at a greater depth. In contrast, the increase in saturated soil permeability of the root zone of the upper layer would provide benefit in terms of soil erosion control by reducing the runoff.

### Influence of roots on soil aggregate stability (SAS)

Figure 17 shows the variation of SAS with plant age for three distinct site locations. Error bars for the SAS have been constructed corresponding to the 95% confidence interval [40]. SAS values in the root zone (UR) samples are higher as compared to the other two locations (UA and UB). This confirms the root exudation explanation presented earlier. During the exudation process, it releases a polymeric gel, which decrease the mobility or clay colloids [19], and this gives rise to the strength and cohesiveness of soil aggregate resistant to breakdown due to natural or manmade forces [35]. Further, SAS can be used as an indicator that represents the soil resistance to runoff and soil erosion [17].

### Conclusions

Understanding the influence of vegetation on unsaturated soil properties is of great importance when studying about rain-induced shallow landslides and implementing soil bioengineering techniques for slope mitigation. This paper examined the effect of vetiver grass on unsaturated soil properties [i.e., soil–water retention curves (SWRC), saturated permeability] and soil aggregate stability with various root contents and plant ages in bio-engineered slopes in Thailand. The following conclusions can be drawn from the study.

The experimental results exhibited that the vetiver roots have a direct impact on the unsaturated soil properties. Air–entry suction slightly decreased and porosity significantly increased as a result of increase in the root biomass, and subsequent formation of macropores and aggregated soil structure in the root zone (0–15 cm depth). Nevertheless, in the lower layer of the root zone (15–25 cm depth), the air–entry suction increased with root biomass due to the occupancy of soil pores by roots. Saturated volumetric water contents were clearly higher around the roots (in both upper and lower layers) as compared to other locations which indicated the improved water holding capacity. A larger variation was observed in the SWRCs in lower layers due to the intrinsic variability of the soil, although the air–entry suction tended to increase with root biomass.

The soil–water retention curves (SWRCs) were found to be influenced by the void ratio and root biomass. The correlations between the SWRC features (e.g., water–entry suction, residual soil suction, etc.), the void ratio and root biomass were determined using multiple-linear regression analysis. Saturated soil permeability was positively correlated with plant age in the root zone, while below the root zone showed a slightly negative correlation. The upslope and downslope soil samples showed a negative correlation due to the effect of sediment trap. The specific water retention capacity and SAS became higher in the root zone and positively correlated with plant age.

**Acknowledgements** The first author is grateful to the scholarship provided by the Department of Civil Engineering and Faculty of Engineering, Kasetsart University. Valuable assistance provided by the students and staffs at Geotechnical Division of Department of Civil Engineering, Department of Soil Physics, Kasetsart University and Green Ground Solutions, co. Ltd are gratefully acknowledged. Department of Rural Roads is also thanked for allowing the access to their bioengineered sites.

**Author contribution** The manuscript of this paper, even with a minor overlap with text, research objectives, presentation of research data, figures/photographs, tables, research findings, conclusions, etc., has not been submitted to any other journal for simultaneous consideration. Also, no part of this paper manuscript has been published earlier by me/us and others at any publication platform (technical journal, conference proceedings, magazine, newspaper, etc.). The details as reported in this paper are truly my/our unpublished original research work in all aspects. Further, all authors contributed to the study conception and design. Material preparation, data collection and analysis were performed by KR and AJ. The first draft of the manuscript was written by KR and all authors edited and commented on previous versions of the manuscript. All authors read and approved the final manuscript.

### References

- Rahardjo H, Satyanaga A, Hoon K, Sham WL, Aaron Ong CL, Huat BBK, Fasihnikoutalab MH, Asadi A, Rahardjo PP, Jotisankasa A, Thu TM, Viet TT (2017) Slope safety preparedness in southeast Asia for effects of climate change. Slope Saf

- Preparedness Impact Clim Change. <https://doi.org/10.1201/9781315387789>
2. Jotisankasa A, Mairaing W (2010) Suction-monitored direct shear testing of residual soils from landslide-prone areas. *J Geotech Geoenviron Eng* 136(3):533–537
  3. Mairaing W, Jotisankasa A, Soralump S (2012) Some applications of unsaturated soil mechanics in Thailand: an appropriate technology approach. *Geotech Eng J SEAGS AGSSEA* 3(1):1–11
  4. Kankanamge L, Jotisankasa A, Hunsachainan N, Kulathilaka A (2018) Unsaturated shear strength of a Sri Lankan residual soil from a landslide-prone slope and its relationship with soil–water retention curve. *Int J Geosynth Ground Eng*. <https://doi.org/10.1007/s40891-018-0137-7>
  5. Collins BD, Znidarcic D (2004) Stability analyses of rainfall induced landslides. *J Geotech Geoenviron Eng* 130(4):362–372
  6. Jotisankasa A, Tapparnich J (2011) Shear and soil-water retention behaviour of a variably saturated residual soil and its implication on slope stability. In: *Proceedings of the 5th international conference on unsaturated soils*, vol 2, pp 1249–1254
  7. Sundaravel V, Dodagoudar GR (2020) Deformation and stability analyses of hybrid earth retaining structures. *Int J Geosynth Ground Eng*. <https://doi.org/10.1007/s40891-020-00222-1>
  8. Daraei A, Herki BMA, Sherwani AFH, Zare S (2018) Slope stability in swelling soils using cement grout: a case study. *Int J Geosynth Ground Eng*. <https://doi.org/10.1007/s40891-018-0127-9>
  9. Rahardjo H, Santoso VA, Leong EC, Ng YS, Hua CJ (2011) Performance of horizontal drains in residual soil slopes. *Soils Found* 51(3):437–447. <https://doi.org/10.3208/sandf.51.437>
  10. Coppin NJ, Richards IG (1990) *Use of vegetation in civil engineering*. Butterworths, Ciria, pp 23–36
  11. Morgan RP, Rickson RJ (1995) Water erosion control. In: *Slope stabilization and erosion control: a bioengineering approach*. pp 133–190
  12. Jotisankasa A, Mairaing W, Tansamrit S (2014) Infiltration and stability of soil slope with vetiver grass subjected to rainfall from numerical modeling. In: *Proceedings of the 6th international conference on unsaturated soils*. UNSAT, pp 1241–1247
  13. Nguyen TS, Likitlersuang S, Jotisankasa A (2018) Stability analysis of vegetated residual soil slope in Thailand under rainfall conditions. *Environ Geotech* 7(5):338–349. <https://doi.org/10.1680/jenge.17.00025>
  14. Mahannopkul K, Jotisankasa A (2019) Influences of root concentration and suction on *Chrysopogon zizanioides* reinforcement of soil. *Soils Found* 59:500–516. <https://doi.org/10.1016/j.sandf.2018.12.014>
  15. Mahannopkul K, Jotisankasa A (2019) Influence of root suction on tensile strength of *Chrysopogon zizanioides* roots and its implication on bio-slope stabilization. *J Mt Sci* 16(2):275–284. <https://doi.org/10.1007/s11629-018-5134-8>
  16. Elia G, Cotecchia F, Pedone G, Vaunat J, Vardon PJ, Pereira C, Springman SM, Rouainia M, Van Esch J, Koda E, Josifovski J (2017) Numerical modelling of slope–vegetation–atmosphere interaction: an overview. *Q J Eng GeolHydrogeol* 50(3):249–270
  17. Frei M, Böll A, Graf F, Heinemann HR, Springman S (2003) Quantification of the influence of vegetation on soil stability. In: *Proceeding of the international conference on slope engineering*. Department of Civil Engineering, pp 872–877
  18. Ni JJ, Leung AK, Ng CWW (2019) Modelling effects of root growth and decay on soil water retention and permeability. *Can Geotech J* 56(7):1049–1055
  19. Jotisankasa A, Sirirattanachai T (2017) Effects of grass roots on soil-water retention curve and permeability function. *Can Geotech J* 54(11):1612–1622
  20. Ng CWW, Ni JJ, Leung AK, Wang ZJ (2016) A new and simple water retention model for root-permeated soils. *Géotechn Lett* 6(1):106–111
  21. Leung AK, Garg A, Coo JL, Ng CWW, Hau BCH (2015) Effects of the roots of *Cynodon dactylon* and *Schefflera heptaphylla* on water infiltration rate and soil hydraulic conductivity. *Hydrol Process* 29(15):3342–3354
  22. Vergani C, Graf F (2016) Soil permeability, aggregate stability and root growth: a pot experiment from a soil bioengineering perspective. *Ecohydrology* 9(5):830–842
  23. Hengchaovanich D (1998) *Vetiver grass for slope stabilization and erosion control*. Off R Dev Proj Board
  24. Truong P, Van TT, Pinners E (2008) *Vetiver system applications technical reference manual*. The Vetiver Network International
  25. Greenfield JC (2008) *The vetiver system for soil and water conservation*. The Vetiver Network International
  26. Jotisankasa A, Sirirattanachai T, Rattana-areekul C, Mahannopkul K, Sopharat, J (2015) Engineering characterization of Vetiver system for shallow slope stabilization. In: *Proceedings of the 6th International Conference on Vetiver (ICV-6)*. Danang, Vietnam, pp 5–8
  27. Wu Z, Leung AK, Boldrin D, Ganesan SP (2021) Variability in root biomechanics of *Chrysopogon zizanioides* for soil eco-engineering solutions. *Sci Total Environ* 776(1):145943
  28. Leung AK, Boldrin D, Liang T, Wu ZY, Kamchoom V, Bengough AG (2018) Plant age effects on soil infiltration rate during early plant establishment. *Geotechnique* 68(7):646–652
  29. Tarawneh B, Al Bodour W, Masada T (2018) Inspection and risk assessment of mechanically stabilized earth walls supporting bridge abutments. *J Perform Constr Facil* 32(1):04017131
  30. Papadopoulos A, Bird NRA, Whitmore AP, Mooney SJ (2009) Investigating the effects of organic and conventional management on soil aggregate stability using X-ray computed tomography. *Eur J Soil Sci* 60(3):360–368
  31. Jotisankasa A (2010) *Manual for user of KU tensiometer*. Geotechnical Innovation Laboratory. Department of Civil Engineering, Faculty of Engineering, Kasetsart University
  32. Barus RMN, Jotisankasa A, Chairaprakaikeow S, Sawangsuriya A (2019) Laboratory and field evaluation of modulus–suction–moisture relationship for a silty sand subgrade. *Transp Geotech* 19:126–134
  33. Lu N, Likos WJ (2004) *Unsaturated soil mechanics*. Wiley, New Jersey
  34. GdeFN G, Fredlund DG (2004) Soil–water characteristic curve equation with independent properties. *J Geotech Geoenviron Eng ASCE* 130(2):209–212
  35. Phocharoen Y, Aramrak S, Chittamart N, Wisawapipat W (2018) Potassium influence on soil aggregate stability. *Commun Soil Sci Plant Anal* 49(17):2162–2174
  36. Böhm W (1979) *Methods of studying root systems*, vol 33. Springer, New York
  37. Hillel D, Hatfield JL (2005) *Encyclopedia of soils in the environment*, vol 3. Elsevier, Amsterdam
  38. Rahardjo H, Satyanaga A, Leong EC, Santoso VA, Ng YS (2014) Performance of an instrumented slope covered with shrubs and deep-rooted grass. *Soils Found* 54(3):417–425
  39. Head KH, Epps R (2011) *Manual of soil laboratory testing*, vol 2. Permeability, shear strength and compressibility test
  40. Clewer AG, Scarisbrick DH (2013) *Practical statistics and experimental design for plant and crop science*. Wiley, New York
  41. Ghestem M, Sidle RC, Stokes A (2011) The influence of plant root systems on subsurface flow: implications for slope stability. *Bioscience* 61(11):869–879